

# PHYSICAL REVIEW B

## CONDENSED MATTER AND MATERIALS PHYSICS

THIRD SERIES, VOLUME 58, NUMBER 18

1 NOVEMBER 1998-II

### RAPID COMMUNICATIONS

*Rapid Communications are intended for the accelerated publication of important new results and are therefore given priority treatment both in the editorial office and in production. A Rapid Communication in Physical Review B may be no longer than four printed pages and must be accompanied by an abstract. Page proofs are sent to authors.*

#### Thermal and nonthermal melting of gallium arsenide after femtosecond laser excitation

K. Sokolowski-Tinten, J. Bialkowski, and M. Boing

*Institut für Laser- und Plasmaphysik, Universität-GHS-Essen, D-45117 Essen, Germany*

A. Cavalleri

*Institut für Laser- und Plasmaphysik, Universität-GHS-Essen, D-45117 Essen, Germany  
and INFN, Dipartimento di Elettronica, Università di Pavia, Via Ferrata 1, 27100 Pavia, Italy*

D. von der Linde

*Institut für Laser- und Plasmaphysik, Universität-GHS-Essen, D-45117 Essen, Germany*

(Received 19 March 1998; revised manuscript received 6 July 1998)

Thermal- and nonthermal melting in gallium arsenide after femtosecond laser excitation has been investigated by means of time resolved microscopy. Electronic melting within a few hundred femtoseconds is observed for rather strong excitation and the data reveal a distinct threshold fluence of  $150 \text{ mJ/cm}^2$  for this nonthermal process. Below that threshold melting occurs on a 100 ps time scale and is of thermal nature. Using a simple numerical model we describe this type of the phase transition as heterogeneous melting under strongly overheated conditions. [S0163-1829(98)51142-3]

Femtosecond laser induced phase transitions in covalently bonded semiconductors have been extensively studied during the past decade. Time resolved optical experiments on silicon,<sup>1-3</sup> gallium arsenide,<sup>3-6</sup> indium antimonide,<sup>7</sup> and carbon<sup>8</sup> clearly demonstrate the existence of a nonthermal, ultrafast melting process upon irradiation with subpicosecond pulses. As first proposed by van Vechten<sup>9</sup> to explain nanosecond laser annealing of semiconductors, ultrafast melting originates from a destabilization of the lattice in the presence of a very dense  $e-h$  plasma. Theoretical studies<sup>10-12</sup> further clarified the nature of the process and set a lower limit of approximately  $10^{22} \text{ carriers/cm}^3$  for the induced lattice instability. Such a high carrier concentration can only be attained by sub-ps laser excitation. At lower carrier densities, however, thermal effects are also important. In particular, it has been shown<sup>13</sup> that for relatively weak femtosecond excitation just above the melting threshold the solid-liquid phase transition is a slow, thermal process occurring by nucleation and growth.

In this communication we present a time resolved study of femtosecond laser induced melting in gallium arsenide,

emphasizing the fluence dependence of the phase transformation. Our data provide clear evidence of competition between classical thermal and ultrafast electronic melting, revealing a distinct threshold fluence for the latter process.

Melting of gallium arsenide is experimentally indicated by a large increase of the reflectivity due to the transition from the semiconducting solid to the metallic liquid phase. Therefore most of the reported experimental work relies on reflectivity measurements using traditional pump-probe techniques. Such experiments provide a space integrated information over an inhomogeneously excited area which may mask details of the reflectivity evolution of the surface. Using time resolved microscopy<sup>14</sup> we obtain the necessary space resolution, thus avoiding spatial averaging effects and providing a richer body of information on the time and the fluence dependence of the melting process. In particular the Gaussian intensity distribution of the focused pump pulse results in a continuous variation of the excitation conditions across the sample surface. Therefore, a single snapshot picture of the illuminated area contains information over an extended range of fluences.

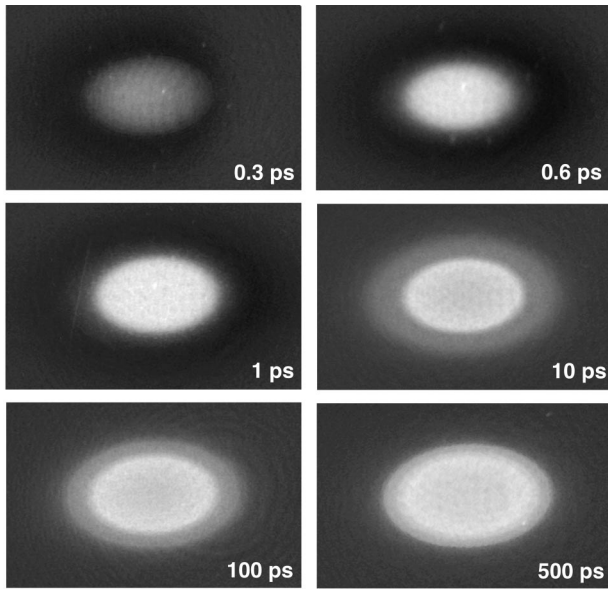


FIG. 1. Pictures of a (100)-GaAs surface at different times after exposure to the pump pulse (pump fluence  $210 \text{ mJ/cm}^2$ ).

Optically polished wafers of single crystalline gallium arsenide (100) were irradiated with 100 fs light pulses at 620 nm provided by a 10 Hz-amplified colliding-pulse, passively mode-locked dye-laser (rhodamine 6G/DODCI). Combining standard pump-probe techniques and optical microscopy the reflectivity of the surface was monitored with both 100 fs temporal and micrometer spatial resolution. A strong pump pulse (p-pol., angle of incidence  $45^\circ$ ) excited the sample and a time delayed probe pulse (s-pol., normal incidence) replaced standard illumination in an optical microscope. The optical micrographs were recorded with a charged coupled device detector and a computer controlled video digitizer. In order to provide a fresh surface for each pump pulse, the wafers were moved between two consecutive exposures.

A typical sequence of micrographs, covering a period of 500 ps following the initial deposition of laser energy, can be appreciated in Fig. 1. The maximum fluence in the center of the spot is  $210 \text{ mJ/cm}^2$ . Due to the large angle of  $45^\circ$  between the pump and the probe beam, the actual delay depends on the spatial coordinate along the horizontal axis of the images ( $100 \text{ fs}/42 \mu\text{m}$ ), but the delay is constant in the vertical direction (zero delay in Fig. 1 is referred to the center of the spot). In the center of the spot, corresponding to maximum fluence, the reflectivity rises within a few hundred femtoseconds, indicating the above mentioned ultrafast electronic melting process. By contrast, in the low fluence regions at the periphery of the excited area the increase of reflectivity takes a few hundred picoseconds to develop. Such time scale, significantly longer than the time needed for energy relaxation,<sup>15</sup> evidences the thermal nature of the process.

To quantitatively follow the evolution of the reflectivity we have plotted in Fig. 2 vertical cross sections of the pictures shown in Fig. 1. Due to the Gaussian intensity profile of the focused pump beam (thin solid curve in Fig. 2) different spatial locations on the sample represent the behavior of the reflectivity for different pump fluences. At very early delay times (300 fs) the reflectivity exhibits a continuous

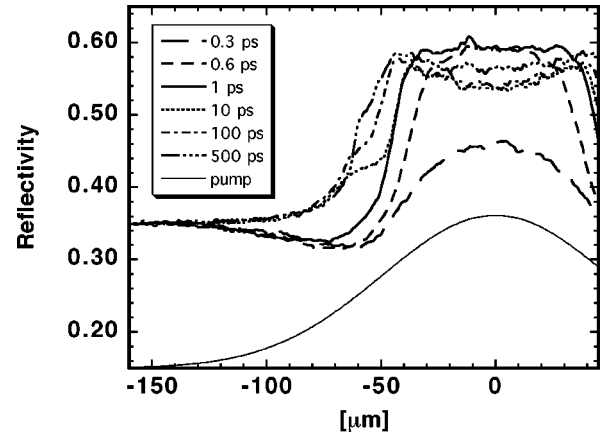


FIG. 2. Vertical cross sections of the snapshot pictures shown in Fig. 1: Reflectivity as a function of the distance to center of the excited spot (fluence dependence). The bottom (thin) solid curve represents the spatial intensity distribution of the focused pump beam.

variation with fluence. An increase in reflectivity is observed for the higher fluences (center of spot) and a decrease for lower fluences (periphery of the spot). During the following few hundred femtoseconds the shape of the reflectivity profiles changes substantially. In approximately one picosecond the initial smooth variation of reflectivity develops into a fluence independent, flat-top profile ( $R=0.6$ ) with a relatively steep drop approximately  $45 \mu\text{m}$  from the center of the spot (corresponding to a fluence of  $150 \text{ mJ/cm}^2$ ). The profiles measured for 10, 100, and 500 ps show the behavior at later time delays. Apparently the size of the initially formed high reflectivity area does *not* increase during the following 10–20 ps, as can be seen particularly well at  $\Delta t = 10 \text{ ps}$ . For fluences slightly below  $150 \text{ mJ/cm}^2$  it takes instead nearly 100 ps for the reflectivity to rise to a level comparable to that observed at higher fluences after only a few hundred femtoseconds. In the center of the spot the reflectivity decreases on a 10–100 ps time scale,<sup>16</sup> eventually returning to the maximum value of  $R=0.6$  in approximately one nanosecond (data not shown here).

The smooth reflectivity profile observed at very early delay times can be readily explained by the optical properties of the initially excited electron-hole plasma. For lower fluences the electron-hole density stays below the critical density<sup>18</sup> causing a decrease in reflectivity. For higher fluences the plasma density exceeds the critical density giving rise to an increased reflectivity.

The observation of a flat-top reflectivity profile for  $\Delta t > 1 \text{ ps}$ , instead, cannot be related to the excited electron-hole plasma. Such fluence independent increase of the reflectivity towards a value close to that expected for liquid gallium arsenide<sup>19</sup> indicates the formation of liquid material over a layer which is thicker than the penetration depth of the probe pulse radiation ( $\approx 20\text{--}30 \text{ nm}$ ). Moreover, the sharp boundary of this area reveals the existence of a distinct threshold ( $150 \text{ mJ/cm}^2$ ) for the occurrence of ultrafast melting. In the frame of the theoretical models mentioned in the introduction<sup>10–12</sup> nonthermal melting is due to instability of the crystal lattice in the presence of a dense electron-hole plasma. If the plasma density exceeds a critical value ( $\approx 10^{22} \text{ cm}^{-3}$ , 10% of the whole valence population)

the transformation to the disordered liquid state is possible within a few vibrational periods. This process occurs *homogeneously* wherever the stability limit is exceeded. The excited volume is given by the absorption depth of the pump in the *solid*, which in our case corresponds to approximately 250 nm. Therefore the stability limit can be reached simultaneously over a depth of several tens of nanometers, much larger than the skin depth of the probe in the *liquid*. Note that the precise determination of the threshold for nonthermal melting emphasizes the advantages of our space-resolved measurement technique. In a normal pump-probe setup this threshold would have been masked by space-averaging effects due to the finite size of the probe beam.

Outside the nonthermally molten area the dynamics of the phase transformation is substantially different. The evolution of reflectivity for lower fluences is characterized by a fast rise during the first 5–10 ps ( $\approx 1/3$  of the total reflectivity rise), and a much slower, continuous increase to the final value of the liquid, which needs hundreds of picoseconds. This behavior is comparable to that observed in picosecond laser melting experiments.<sup>20</sup> In the picosecond case the phase transformation proceeds under strongly overheated conditions,<sup>21</sup> i.e., the temperature of the solid exceeds the equilibrium melting temperature. Melting occurs by *heterogeneous* nucleation of the liquid phase, which starts at the sample surface.<sup>22</sup> The rise in reflectivity is interpreted in terms of the progressively increasing thickness of the metallic liquid layer in front of the semiconducting solid substrate. The melting rate is determined by the velocity of the solid-liquid interface and ultimately limited to the speed of sound.

To model the thermal melting process after femtosecond excitation we performed computer simulations based on a numerical solution of the one-dimensional heat-flow equation. Because the lateral length scales (pump beam diameter) are much larger than the typical length scales perpendicular to the surface (pump absorption depth) lateral heat diffusion can be neglected and a one-dimensional description is sufficient. We did not model the optical excitation process and the initial stage of relaxation in the electronic system. Due to the fast energy relaxation we assumed instead that within a few picoseconds after excitation a certain temperature distribution is established in the *solid* phase of the material. This distribution is determined by the effective pump absorption depth and by carrier diffusion processes. It is characterized by strong overheating of the solid phase, because a certain amount of energy, corresponding to the necessary latent heat of fusion, has to be initially stored in the solid. As in the picosecond case melting is assumed to start at the surface by heterogeneous nucleation. The velocity of the solid-liquid interface is a function of its temperature (*interface response function*, IRF). The thickness of the liquid layer increases as long as the solid is overheated, whereas resolidification takes place when the interface temperature drops below the melting point (undercooling of the liquid). We choose a phenomenological form of the IRF (Ref. 22) with parameters which were inferred from the interface velocities observed in picosecond laser melting experiments.<sup>23</sup> The temperature dependence of the thermophysical properties of the material is kept into account by means of extrapolating the known dependencies<sup>24</sup> to the overheated state of the solid. It should be noted that a detailed *quantitative* description of the ex-

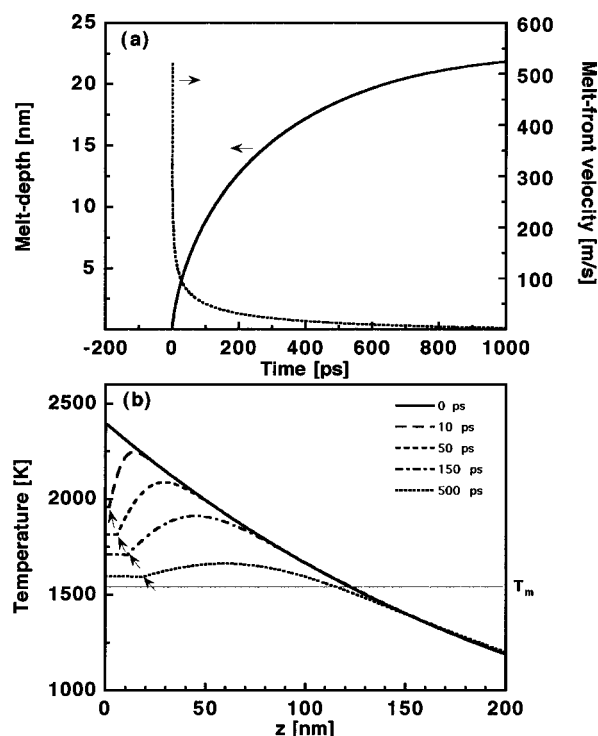


FIG. 3. Results of model calculations for an initial maximum surface temperature of 2.400 °K: (a) melt depth and melt-front velocity as a function of time; (b) temperature distributions perpendicular to the sample surface for different times after excitation. The melting temperature  $T_m$  is marked by the horizontal line, the position of the solid-liquid interface by small arrows.

perimental data is far beyond the capabilities of our model due to the various assumptions and restrictions. Nevertheless we will show that the model is capable to *qualitatively* account for the observed time evolution of the reflectivity.

Typical results of the calculations are depicted in Figs. 3(a) and 3(b). Fig. 3(a) shows melt depth and melt-front velocity as a function of time, whereas in Fig. 3(b) the spatial temperature profiles (perpendicular to the sample surface) are plotted for different times after excitation. The main qualitative features of the experimental observations are well reproduced by the calculations. Initially the velocity of the melt front is extraordinary high (a few hundred m/s). This explains the observed increase of reflectivity during the first 10 ps. Later the movement of the phase boundary slows down significantly and the interface velocity drops below 50 m/s. In the calculations it takes more than a nanosecond to reach the maximum melt depth, again in good qualitative agreement with the experimental data. The analysis of the spatial temperature distributions shown in Fig. 3(b) explains this behavior. Initially the material at the surface is strongly overheated. This leads to rapid melting of the near surface layer and to a correspondingly high velocity of the liquid-solid interface [marked by arrows in Fig. 3(b)]. Simultaneously the temperature is reduced (by more than 400 °K after 10 ps) due to the consumption of latent heat during the melting process, and the melt-front velocity drops accordingly. It should be noted that, due to the moderate temperature gradient in the initial distribution, heat conduction into the bulk is negligible. The change of the temperature in the vicinity of the melt front at early times is only related to

melting and to the concomitant consumption of latent heat. The spatial temperature distributions are characterized by large *positive* temperature gradients ( $\partial T/\partial z > 0$ ) behind the solid-liquid interface, resulting in a temporary reversal of the direction of the heat flow. Energy is transferred from the deeper parts of the sample to the phase boundary causing the slow, continuous increase of the molten layer thickness.

Recently Huang *et al.*<sup>6</sup> reported on temporally and spectrally resolved measurements of the dielectric function of femtosecond excited gallium arsenide. Depending on excitation strength they identified different regimes in the time evolution of the optical properties. For high fluences their data show a fast transition from semiconducting to metallic behavior indicating the known nonthermal melting of the material. For somewhat lower fluences they interpreted the changes of the dielectric function observed during the first 10 ps as an indication for lattice disordering *without* the semiconductor-to-metal transition associated with melting. We suggest that the spectra measured by Huang and co-workers after a few picoseconds represent the optical prop-

erties of the strongly overheated solid. It should be noted that during the early stage of thermal, heterogeneous melting extremely inhomogeneous temperature distributions are expected [Fig. 3(b), 10 and 50 ps] and therefore any optical measurement averages over a layer with strongly varying optical constants.

In summary we have studied thermal and nonthermal melting of gallium arsenide after femtosecond laser excitation. For higher excitation fluences homogeneous, electronic melting within a few hundred femtoseconds is observed. This nonthermal process exhibits a distinct threshold fluence of 150 mJ/cm<sup>2</sup>. Below that threshold the data indicate heterogeneous melting under strongly overheated conditions. Extraordinary high melt-front velocities and nonmonotonic temperature distributions are unique features of this rapid thermal process.

K.S.T. acknowledges support by the Flughafen Frankfurt Main foundation and by the University of Essen (Forschungspool). A.C. acknowledges support by the European Community (Human Capital and Mobility).

- 
- <sup>1</sup>C. V. Shank, R. Yen, and C. Hirlimann, *Phys. Rev. Lett.* **50**, 454 (1983); **51**, 900 (1983).
- <sup>2</sup>H. W. K. Tom, G. D. Aumiller, and C. H. Brito-Cruz, *Phys. Rev. Lett.* **60**, 1438 (1988).
- <sup>3</sup>K. Sokolowski-Tinten, J. Bialkowski, and D. von der Linde, *Phys. Rev. B* **51**, 14 186 (1995).
- <sup>4</sup>S. V. Govorkov, T. Schröder, I. L. Shumay, and P. Heist, *Phys. Rev. B* **46**, 6864 (1992).
- <sup>5</sup>P. Saeta, J.-K. Wang, Y. Siegal, N. Bloembergen, and E. Mazur, *Phys. Rev. Lett.* **67**, 1023 (1991); E. N. Glezer, Y. Siegal, L. Huang, and E. Mazur, *Phys. Rev. B* **51**, 9589 (1995).
- <sup>6</sup>L. Huang, J. P. Callan, E. N. Glezer, and E. Mazur, *Phys. Rev. Lett.* **80**, 185 (1998).
- <sup>7</sup>I. L. Shumay and U. Höfer, *Phys. Rev. B* **53**, 15 878 (1996).
- <sup>8</sup>D. H. Reitze, H. Ahn, and M. C. Downer, *Phys. Rev. B* **45**, 2677 (1992).
- <sup>9</sup>J. A. van Vechten, R. Tsu, and F. W. Saris, *Phys. Lett.* **74A**, 422 (1979).
- <sup>10</sup>P. Stampfli and K. H. Bennemann, *Phys. Rev. B* **42**, 7163 (1990); **46**, 10 686 (1992); **49**, 7299 (1994).
- <sup>11</sup>P. L. Silvestrelli, A. Alavi, M. Parrinello, and D. Frenkel, *Phys. Rev. Lett.* **77**, 3149 (1996).
- <sup>12</sup>J. S. Graves and R. E. Allen (unpublished).
- <sup>13</sup>K. Sokolowski-Tinten, H. Schulz, J. Bialkowski, and D. von der Linde, *Appl. Phys. A: Solids Surf.* **53**, 227 (1991).
- <sup>14</sup>M. C. Downer, R. L. Fork, and C. V. Shank, *J. Opt. Soc. Am. B* **4**, 595 (1985).
- <sup>15</sup>N. Bloembergen, in *Beam-Solid Interactions and Phase Transformations, 1985*, edited by H. Kurz, G. L. Olson, and J. M. Poate, MRS Symposia Proceedings No. 51 (Materials Research Society, Pittsburgh, 1986), p. 3.
- <sup>16</sup>The magnitude of the observed decrease in reflectivity is fluence dependent. It is probably related to the temperature dependence of the optical properties of the liquid material, similar to what has been observed in liquid silicon (Ref. 17).
- <sup>17</sup>J. Boneberg, O. Yavas, B. Mierswa, and P. Leiderer, *Phys. Status Solidi B* **174**, 295 (1992).
- <sup>18</sup>The critical density is given by  $N_{cr} = (2\pi c/\lambda)^2 (m^* \epsilon_0 \epsilon / e^2)$ , where  $c$  is the speed of light,  $\lambda$  the probe pulse wavelength,  $m^*$  the optical effective mass, and  $\epsilon$  the dielectric constant.
- <sup>19</sup>No reliable data exist on the optical properties of l-GaAs. The Drude model, treating l-GaAs as a pure free-electron metal, has been used to fit transient reflectivities observed in our previous laser melting experiments (Ref. 13). From these fittings we expect a normal-incidence reflectivity at 620 nm of approximately 0.62, close to the observed value of 0.6.
- <sup>20</sup>B. Danielzik, P. Harten, K. Sokolowski-Tinten, and D. von der Linde, in *Fundamentals of Beam-Solid Interactions and Transient Thermal Processing*, edited by M. J. Aziz, L. E. Rehn, and B. Stritzker, MRS Symposia Proceedings No. 100 (Materials Research Society, Pittsburgh, 1988), p. 471.
- <sup>21</sup>N. Fabricius, P. Hermes, D. von der Linde, A. Pospieszczyk, and B. Stritzker, *Solid State Commun.* **58**, 239 (1986).
- <sup>22</sup>F. Spaepen and D. Turnbull, in *Laser Annealing of Semiconductors*, edited by J. M. Poate and J. W. Mayer (Academic, New York, 1985), p. 15.
- <sup>23</sup>We choose the following functional relationship between the interface velocity  $v$  and the interface temperature  $T$ :
- $$v(T) = v_0 e^{(-T_0/T)} [e^{(L_a/k_B T_m)(T-T_m)/T} - 1].$$
- $T_m$  and  $L_a$  denote the melting temperature and the latent heat of fusion (per GaAs molecule), respectively, and  $v_0$  and  $T_0$  (unknown) parameters determined by microscopical material properties (Ref. 22). With  $v_0 = 160$  m/s and  $T_0 = 2550$  °K this IRF gives a reasonable approximation of the maximum interface velocities (melting and resolidification) observed in picosecond experiments (Ref. 20).
- <sup>24</sup>J. S. Blakemore, *J. Appl. Phys.* **53**, R123 (1982).